Earthquakes and Structures, *Vol. 8, No. 3 (2015) 591-617*
DOI: http://dx.doi.org/10.12989/eas.2015.8.3.591

Rotational capacity of shallow footings and its implication on SSI analyses

Carlos A. Blandon[1a], J. Paul Smith-Pardo[*2] and Albert Ortiz[3b]

[1]*Department of Civil Engineering, Escuela de Ingenieria de Antioquia, Medellin, Colombia*
[2]*Department of Civil and Environmental Engineering, Seattle University, Seattle, WA, USA*
[3]*Department of Civil and Environmental Engineering, University of South Carolina, Columbia, SC, USA*

(Received November 13, 2013, Revised June 15, 2014, Accepted July 15, 2014)

Abstract. Standards for seismic assessment and retrofitting of buildings provide deformation limit states for structural members and connections. However, in order to perform fully consistent performance-based seismic analyses of soil-structure systems; deformation limit states must also be available for foundations that are vulnerable to nonlinear actions. Because such limit states have never been established in the past, a laboratory testing program was conducted to study the rotational capacity of small-scale foundation models under combined axial load and moment. Fourteen displacement-controlled monotonic and cyclic tests were performed using a cohesionless soil contained in a 2.0×2.0×1.2 m container box. It was found that the foundation models exhibited a stable hysteretic behavior for imposed rotations exceeding 0.06 rad and that the measured foundation moment capacity complied well with Meyerhof's equivalent width concept. Simplified code-based soil-structure analyses of an 8-story building under an array of strong ground motions were also conducted to preliminary evaluate the implication of finite rotational capacity of vulnerable foundations. It was found that for the same soil as that of the experimental program foundations would have a deformation capacity that far exceeds the imposed rotational demands under the lateral load resisting members so yielding of the soil may constitute a reliable source of energy dissipation for the system.

Keywords: soil-structure interaction (SSI); limit states; foundation rotation; nonlinear analysis

1. Introduction

The performance of a building under major ground motions depends on the balance between stiffness, strength, and the deformation capacity of its structural members and connections. Although the importance of deformation capacity in performance-based frameworks has been recognized for several decades, there still appears to be a major disconnect in practice when it comes to soil-foundation systems as current design standards for seismic assessment and rehabilitation of buildings (ASCE 41-06) only recognize the finite stiffness and the finite bearing capacity of foundations with no consideration to their deformation capability.

The lack of information in this regard could be related to the fact that structural engineers

∗Corresponding author, Professor, E-mail: smithjh@seattleu.edu
[a]Professor, E-mail: pfcblandon@eia.edu.co
[b]M.Sc., E-mail: arortiz@udem.edu.co

http://www.techno-press.org/?journal=eas&subpage=7 ISSN: 2092-7614 (Print), 2092-7622 (Online)

typically design foundations to be capacity-protected so they do not expect plastification of the supporting soil to occur. Geotechnical engineers, on the other hand, commonly proportion foundations based on strength and stiffness of the supporting soil with no regard to its ductility. However, deformation capacity can be relevant to the seismic performance of a building when its foundations are prone to uplifting and/or to reaching the bearing capacity of the supporting soil during a strong ground motion. Vulnerable foundations can exist when a building, deemed to be inadequate by the standards of current seismic codes, is rehabilitated through the installation of shear walls and modifications of the footings are not possible. Under this circumstance the original foundations may not have the strength to develop the large moment demands imposed by the strong and stiff retrofitting members (Smith-Pardo 2008) so that the extent of rotation capacity that the footings can sustain before losing their ability to carry load becomes critical to the seismic performance of the building.

Foundation deformation capacity can be advantageous to the seismic performance of structures because of the energy dissipation associated with yielding of the soil and period shifting due to rocking and uplifting, however, drift demands may be more significant (Gajan *et al*. 2008, Harden and Hutchinson 2009, Ugalde *et al*. 2010) and exceed acceptable design levels. In order to investigate these issues, the main focus of this paper is to present the results from an experimental program aimed at determining the rotational capacity of shallow foundations and studying its implications on the seismic response of structures subjected to major seismic excitation.

2. Simplified soil-structure interaction

The study of soil-structure interaction problems can be traced back over a century ago when Lamb (1904) first described the response of a semi-infinite elastic media under point loads. Relevant experimental programs took place decades later (Hall 1967, Parmelee 1967, Parmelee *et al*. 1968) but were limited to the linear range of response for the supporting soil. Recent formulations are significantly more robust -having the capability to capture the coupled nonlinear material and uplift response at the soil-foundation interface- and supported by extensive monotonic, dynamic and centrifuge tests. In these modern approaches, soil-structure interaction is generally formulated either on the basis of macro-models (Cremer *et al*. 2001, Grange *et al*. 2009,

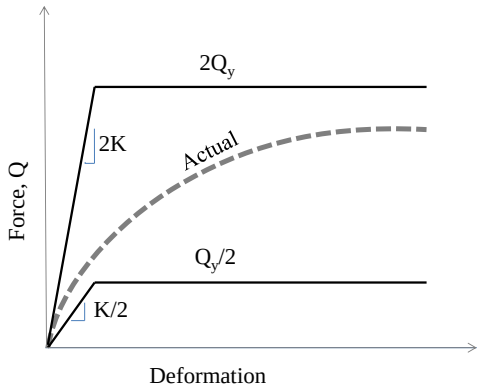

Fig. 1 Foundation force-displacement relations in current design provisions

Chatzigogos *et al*. 2009) or on the basis of beam-on-nonlinear-Winkler models (Raychowdhury 2008, Harden and Hutchinson 2009, Gajan *et al*. 2010).

While recent nonlinear soil-foundation formulations are amenable for research, design guidelines still recommend the use of simple elasto-plastic force-deformation relations because of the inherent difficulty to reliably determine soil properties and the variability of site conditions found in engineering practice. In order to recognize such uncertainties, evaluation of lower and upper bound values for stiffness and strength of the soil is required in ASCE 41-06 (2007) to evaluate the sensitiveness of structural response to soil parameters. As illustrated in Fig. 1, the actual force-displacement relation characterizing a foundation is generally accepted to fall within the elasto-plastic relations obtained by multiplying and dividing by two the expected elastic foundation stiffness (K) and strength (Q_y).

ASCE 41-06 expressions for the static stiffness of shallow foundations were first derived by Pais and Kausel (1988) using elastic half space theory. For the particular case of rocking about the short axis, for example, the rotational stiffness of a shallow rectangular foundation is given by

$$K_\theta = \frac{M}{\theta} = \frac{GB^3}{1-\nu}\left[0.4\left(\frac{L}{B}\right)+0.1\right] \tag{1}$$

where B is the dimension of the footing in the plane of the applied moment; L is the dimension of the footing perpendicular to the plane of applied moment; and G and ν are the effective shear modulus and Poisson's ratio of the supporting soil.

A conventional Winkler formulation (Winkler 1867), in which settlements are assumed to be small and proportional to contact stresses, can alternatively be used to calculate the rotational stiffness of a shallow foundation as follows

$$K_\theta = \frac{M}{\theta} = (K_{S0}B)L\frac{B^2}{12}, \qquad \text{for } e/B \le 1/6 \tag{2a}$$

$$K_\theta = \frac{M}{\theta} = (K_{S0}B)L\frac{B^2}{12}\left[\frac{9}{2}\left(\frac{e}{B}\right)\left(\frac{1}{2}-\frac{e}{B}\right)^2\right], \qquad \text{for } e/B > 1/6 \tag{2b}$$

where K_{s0} is the soil subgrade modulus, and e is the eccentricity of the axial load. The term $K_{s0}B$ may be taken as the initial slope of the mean stress-vs.-normalized settlement response obtained from concentrically loaded foundations/plates (Fig. 2(a)). Normalization of the settlement has been found to alleviate size effects (Briaud and Gibbens 1994, 1999, Consoli *et al*. 1998, Smith-Pardo and Bobet 2007).

Eqs. (1)-(2) define alternative expressions for the slope of a linear relation between the moment acting on a foundation and the rotation that it induces. In design standards this relation is bounded by the foundation moment capacity, which can be estimated with acceptable degree of accuracy using the equivalent width method introduced by Meyerhof (1953). As illustrated in Fig. 2, the concept is based on the premise that the supporting soil can fully plastify at the same level of contact stress, σ_0, irrespectively of whether the foundation is loaded concentrically or eccentrically.

Establishing equilibrium in the two configurations, the following relation between the concentric loading capacity, P_0, and the eccentric loading capacity, P, can be obtained

$$P = P_0\left[1-\frac{2e}{B}\right] \tag{3}$$

Then, setting e=M/P and rearranging Eq. (3) a simplified expression for the plastic moment capacity of a shallow foundation is obtained

$$M = P_0 e\left[1-\frac{2e}{B}\right], \quad \text{for e=constant} \tag{4a}$$

$$M = \frac{PB}{2}\left[1-\frac{1}{FS_V}\right], \quad \text{for P=constant} \tag{4b}$$

where $FS_v=P_0/P$ is the factor of safety for vertical load.

Admittedly, the equivalent width concept does not obey strict principles of mechanics but it rather consists of a convenient tool that facilitates the design of foundations under combined axial load and moment. Eqs. (2) and (4) can be combined to produce a simplified elastoplastic moment-rotation relation that, similar to current design standards, heuristically accounts for the limited stiffness and the limited bearing capacity of a shallow foundation at the base of a column or shear wall. The resulting relation accounts for two of the three essential aspects to the seismic design of structural systems: stiffness and strength. The third aspect consists of the definition of a finite rotational capacity limit at which the foundation could lose its ability to sustain loads. Because of the difficulty and inherent uncertainties associated to the estimation of the deformation capacity based on fundamental principles, a series of tests were conducted in this study to experimentally determine the rotational capacity of shallow foundations on a cohesionless soil. It is recognized that when the deformation capacity is reached, the contact stress distribution under the foundation is non-uniform and thus inconsistent with the equivalent width method. However, determination of the actual yielding mechanism and the plastic state at failure are beyond the scope of this investigation.

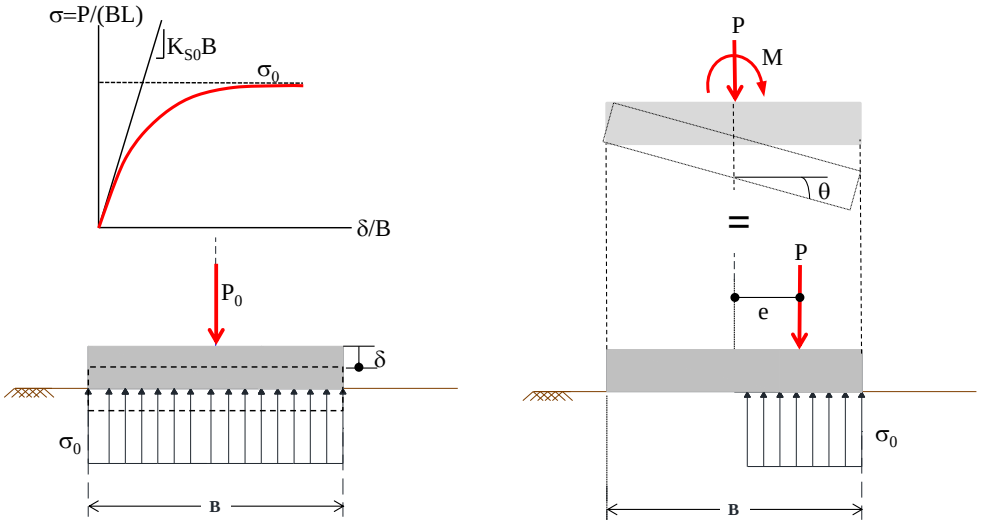

a) Yielding under concentric loading b) Yielding under eccentric loading

Fig. 2 Concentric and eccentric bearing capacity of a shallow foundation

Table 1 Experimental program description

Test	Series	Type	Axial load, P(kN)	Eccentricity, e (mm)
1	I	Monotonic	Varying	0
2		Cyclic		0
3	II	Monotonic	Varying	20
4				33
5				50
6		Cyclic		20
7				33
8				50
9	III	Monotonic	6	Varying
10			18	
11			24	
12		Cyclic	6	
13			18	
14			24	

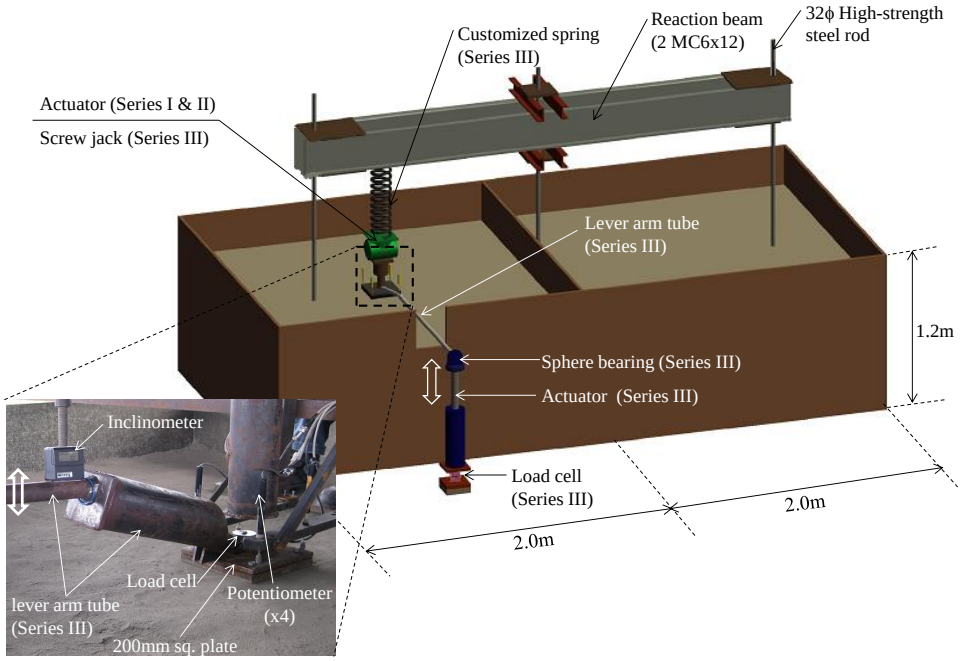

Fig. 3 General test setup

3. Test program

As summarized in Table 1, the test program was divided in series depending on the load pattern that was applied to a 200 mm-square×12 mm-thick steel plate. Series I consisted of concentric

axial loading tests, which define the stiffness ($K_{s0}B$) and strength (P_0) of the foundation and thus provide information to characterize its behavior under combined axial load and moment by means of Eqs. (2) and (4). Series II consisted of constant eccentricity tests in which the applied moment is proportional to the applied axial load. Eccentricities were, e=20, 33, and 50 mm (i.e., B/10, B/6, and B/4) to represent cases where the vertical load falls inside and outside the middle third (kern) of the foundation. Series III consisted of varying moment tests with constant axial loads of P=6, 15, and 24 kN to represent a range of factors of safety ($FS_v=P_0/P$) from about 1.4 to 5.5.

The general test setup and loading apparatus are depicted in Fig. 3 for the constant axial load tests (Series III). A minor modification of this configuration was required for the constant eccentricity tests (Series I and II) as illustrated in Fig. 4.

Two identical wooden containers, each with 2.0×2.0 m plan dimensions and 1.2 m depth, were used to place the soil. The plan dimensions were believed to produce negligible boundary effects because: i) the foundation model was only one tenth of the container size, ii) the flexible wooden container did not appear to deform during the execution of any of the tests, iii) the mode of failure observed during the tests was predominantly local rather than global. In the vertical direction, the contribution to bearing capacity is well-accepted to be provided by the soil within a distance 2B (0.4m); thus confinement effect of the strong floor of the laboratory was also expected to be minimal.

Upon completion of a test, only the upper 450 mm of soil at the surface was removed and transferred to the adjacent container. The soil was placed in layers of 150 mm thickness and was densified by vibro compaction using a 0.45×0.90 m plate compactor that was passed about four times on the surface of each layer. Compaction energy was significant as evidenced by the consistently high density that was measured in the upper 300 mm of soil. After transferring the soil from one container to the other, the 200 mm square footing model, actuator, and measuring devices were also moved. Although only one test was conducted at a given time, this process proved to be efficient since soil removal and soil compaction in preparation for the next test took place simultaneously.

For the constant eccentricity tests (Series I and II), the vertical load was applied to the foundation model by means of a hydraulic actuator reacting against a 3 m-long continuous beam. The reaction beam was spanning within the two wooden container boxes and consisted of two MC6×12 back-to-back steel sections supported by three 32 mm diameter steel rods anchored to the strong floor of the laboratory. The magnitude of the vertical force was measured using a 51 mm miniature compression load cell, while displacements were measured using four linear potentiometers placed at the corners of the foundation model. In order to apply cycles of constant eccentricity, an additional steel beam was used to transfer the load from the hydraulic actuator to the plate as shown in Fig. 4. The auxiliary beam was suspended from the reaction frame through a tensor at one end and further supported by a steel block placed on top of a load cell. The reaction from the steel block became the eccentric load acting on the foundation model. Both, the steel block and load cell were placed at either side of the foundation's center and switched after every cycle.

For the constant axial load tests (Series III), the vertical load was applied first by using a high-precision worm gear jack that acted against a large custom-made spring placed below the reaction beam. The purpose of the spring was to reduce the axial stiffness of the vertical loading system and thus alleviate the variation in the axial load that was induced by the rotation of the footing. The overturning moment was subsequently applied by using a hydraulic actuator against the free end of a 1.5 meter long steel tube bolted to the footing model and cantilevering out the container box

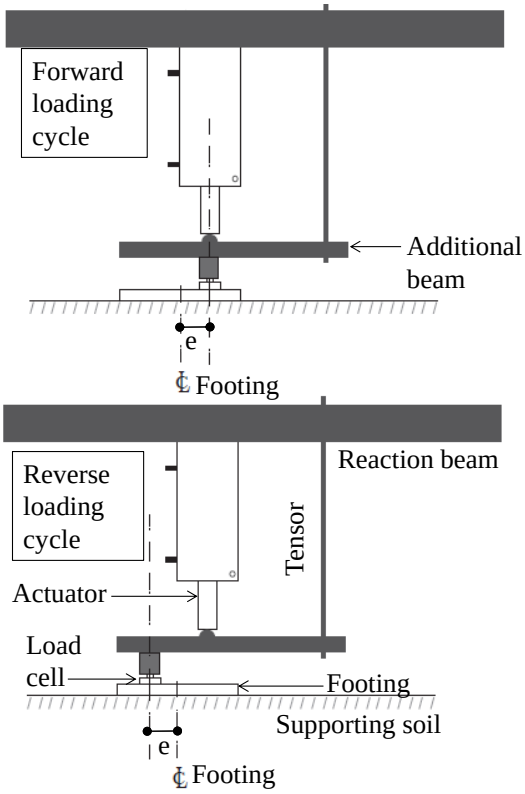

Fig. 4 Setup variation for constant eccentricity tests (Series I and II)

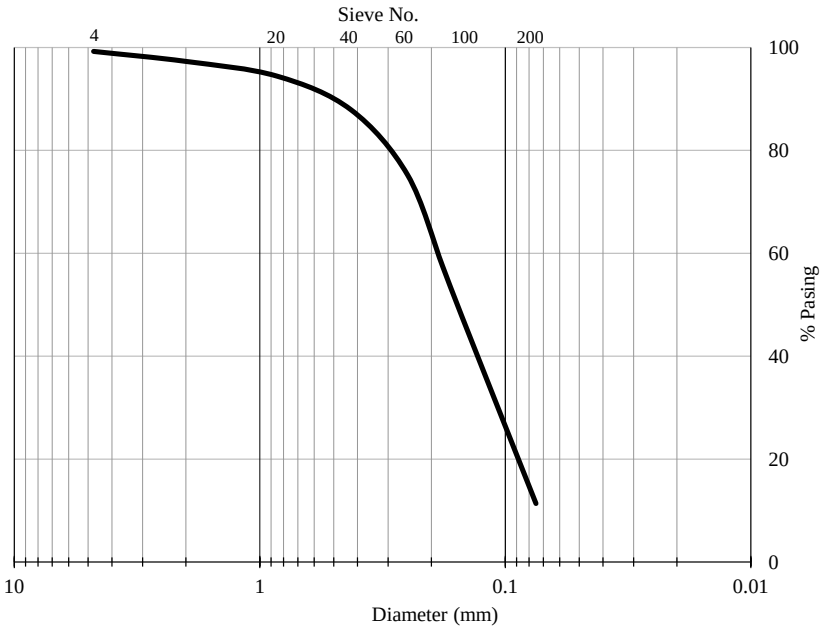

Fig. 5 Particle size distribution of test soil

(Fig. 3). The actuator reacted against a load cell resting on the strong floor and was connected to the level-arm by means of a spherical bearing. The screw jack was manually adjusted during the execution of Series III tests in order to ensure an approximately constant axial load.

The target rotation history imposed to the footing model was controlled using an inclinometer and consisted of single cycles at increasing amplitudes of 0.3, 0.6, 1.0 degrees (0.017 rad) followed by further increments of one degree. Although several cycles would be more representative of earthquake actions, investigation of the effect of this variable on the deformation capacity of foundations has been reserved for future research.

The test soil had 11% of fines and was fairly uniform as evidenced by the narrow particle size distribution shown in Fig. 5. The measured plastic and liquid limits were 24% and 28% respectively. According to the USCS classification (ASTM D2487), the supporting soil was labelled as poorly graded sand with silt (SP-SM). Estimated minimum and maximum dry densities were 1,100 and 1,500 kg/m^3 as obtained by ASTM D4253 and D4254, whereas the specific gravity was 2.75 (ASTM D854). The in-situ relative density of the soil was above 100% which indicates that a significant level of compaction was achieved throughout the experimental program. For every test described in Table 1, density was measured at various locations on the surface of the soil by using the standard Sand-Cone Method (ASTM D1556). The measured density through a depth of 300 mm was consistently between 1,800 and 1,900 kg/m^3. Direct shear tests (ASTM D3080) were also conducted for different levels of compaction and confinement stresses. Using the results from these tests and the soil densities measured in-situ, the internal friction angle was estimated to be around 46^o. Water content (ASTM D2216) varied from about 10% to 5% during the five-month period of the experimental program. The variation was associated to changes in the relative humidity at the site and the fact that the laboratory facility was outdoors. Although suction stresses could influence the stiffness and strength of the soil, these were not evaluated in the current phase of the experimental program.

4. Test results

Fig. 6 shows the settlement (δ) versus axial load (P) response for the monotonic and cyclic concentric load tests of Series I. The application of displacement cycles at low amplitudes produced a significant increase in the bearing capacity, which is believed to be due to the further compaction of the soil upon loading. The large displacement reached before any decay in the load was accompanied by a punching-type mode of failure that started with minor soil bulging around the footing model, followed by surface cracks forming at the corners, and ended with further cracks along the perimeter propagating radially (Fig. 7). This was unexpected given the high relative density of the soil and prompted the execution of additional tests to evaluate the effect of compaction on the mode of failure. It was observed, however, that even for soil layers of only 50 mm (and the same compaction protocol), the global wedging surface did not occur. Regardless of the mode of failure, the attainment of large settlements while maintaining the foundation bearing capacity is a desirable feature in the seismic response of soil-structure systems because soil plastification could become a source of energy dissipation during a strong ground motion.

Two parameters can be extracted from the monotonic test result shown in Fig. 6 to help characterizing the response of the foundation model under a more general loading condition of combined axial load and moment. The parameters are the monotonic peak concentric load capacity, P_0=33 kN, and the initial slope of the force/stress-normalized settlement diagram,

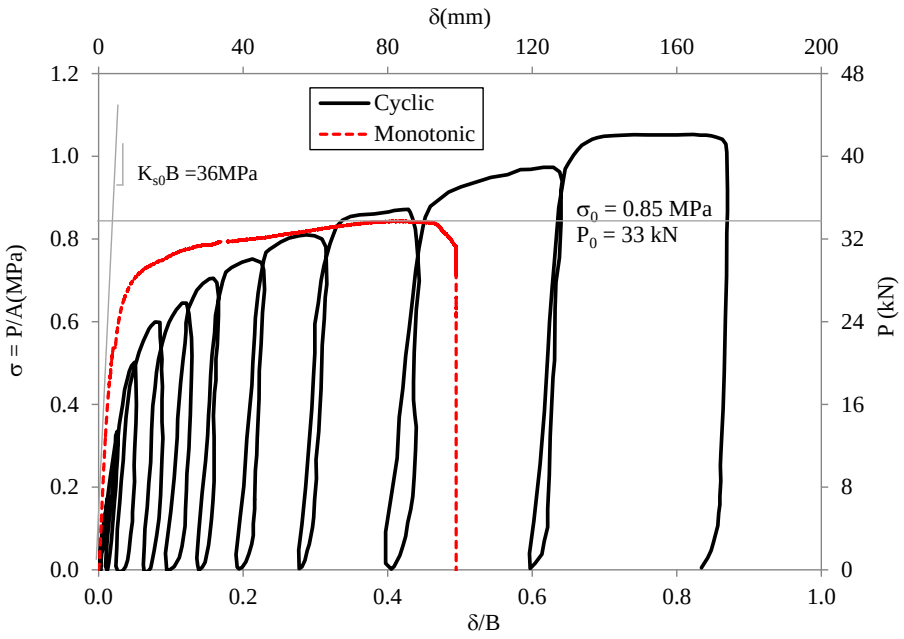

Fig. 6 Settlement response for foundation model under concentric loading

Fig. 7 Punching shear mode of failure in concentric loading test

$K_{s0}B$=36 MPa. These can respectively be used to estimate the initial rotational stiffness, K_0 (for a footing of the same size and in the same soil) based on Eq. (2a) or (2b) and the moment capacity, based on Eq. (4a) or (4b).

By contrast with the concentric load tests, soil bulging was present at the end of the combined axial load and moment tests (Fig. 8). Corresponding measured moment-rotation responses are shown in Figs. 9-10 for the constant eccentricity tests (Series II) and in Figs. 11-12 for the constant axial load tests (Series III). The simplified elastoplastic relationships defined by substitution of

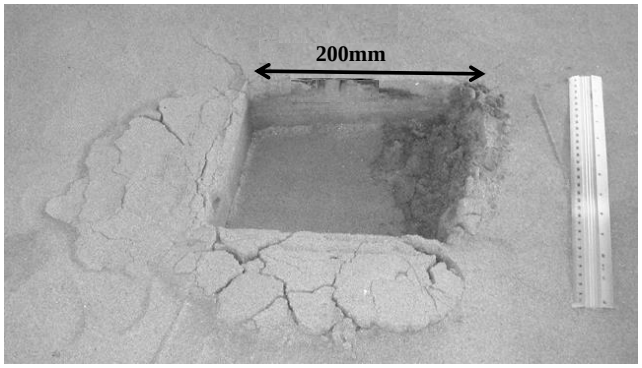

Fig. 8 Mode of failure in combined axial load and moment test (Series II and III)

$K_{s0}B$ and P_0 above into Eqs. (2) and (4) are also included in those figures for comparison purposes. For the monotonic test with constant axial load P=15 kN, potentiometer readings were accidentally lost and only the maximum applied moment was recovered. In addition, an accidental eccentricity between the screw jack and the centerline of the reaction frame took place after the initiation of the cyclic test with constant axial load P=24 kN, which prevented the execution of more load reversals.

Large rotations were observed in test Series II and III before the foundation model started to lose its capability to carry moment. In addition, hysteretic loops were generally wide and stable except for the test with low constant axial load P=6 kN ($FSv=P_0/P=5.5$) which exhibited a pinched moment-rotation response. Uplifting and gapping took place during that particular test as the axial load was insufficient to keep the footing model fully attached to the supporting soil. This observation is consistent with published research in the US and Europe which recognizes FSv as a key parameter delineating the hysteretic curves of foundations under cyclic loading; with higher values of FSv (lower axial load) being associated to a more pinched behavior (Gajan *et al*. 2008). The same feature can also be noticed from Fig. 10, in which the test with largest eccentricity (e = 50 mm) and thus lowest axial load at failure, also exhibits a more pinched response.

For the monotonic tests, the rotational capacity of the foundation model, θ_n, was defined as that for which an increase in the imposed rotation required a reduction in the applied moment. For the cyclic load tests, θ_n was defined as the maximum rotation in a cycle with a peak moment smaller or equal than the peak moment in a previous cycle. The rotational capacity based on these definitions is indicated in the positive quadrant of Figs. 9-12. For the cyclic tests with e=50 mm and P=15 kN, the rotational capacity was not achieved before the tests were stopped so the maximum measured rotation was conservatively reported instead.

Measured foundation rotational capacities are shown in Fig. 13 as a function of the normalized eccentricity (e/B) and in Fig. 14 as a function of the normalized axial load (P/P_0). In order to include the results from constant axial load tests (Series III) in Fig. 13, the eccentricity was calculated as the measured maximum peak moment divided by the axial load. Similarly, in order to include the constant eccentricity tests (Series II) in Fig. 14, the reported axial load was that measured at the maximum peak moment.

Consistent with what can be expected in structural systems, it is observed that the foundation rotational capacities measured in the monotonic tests are generally larger than those measured in the cyclic tests. As the eccentricity increases, the mode of failure of the foundation would tend to

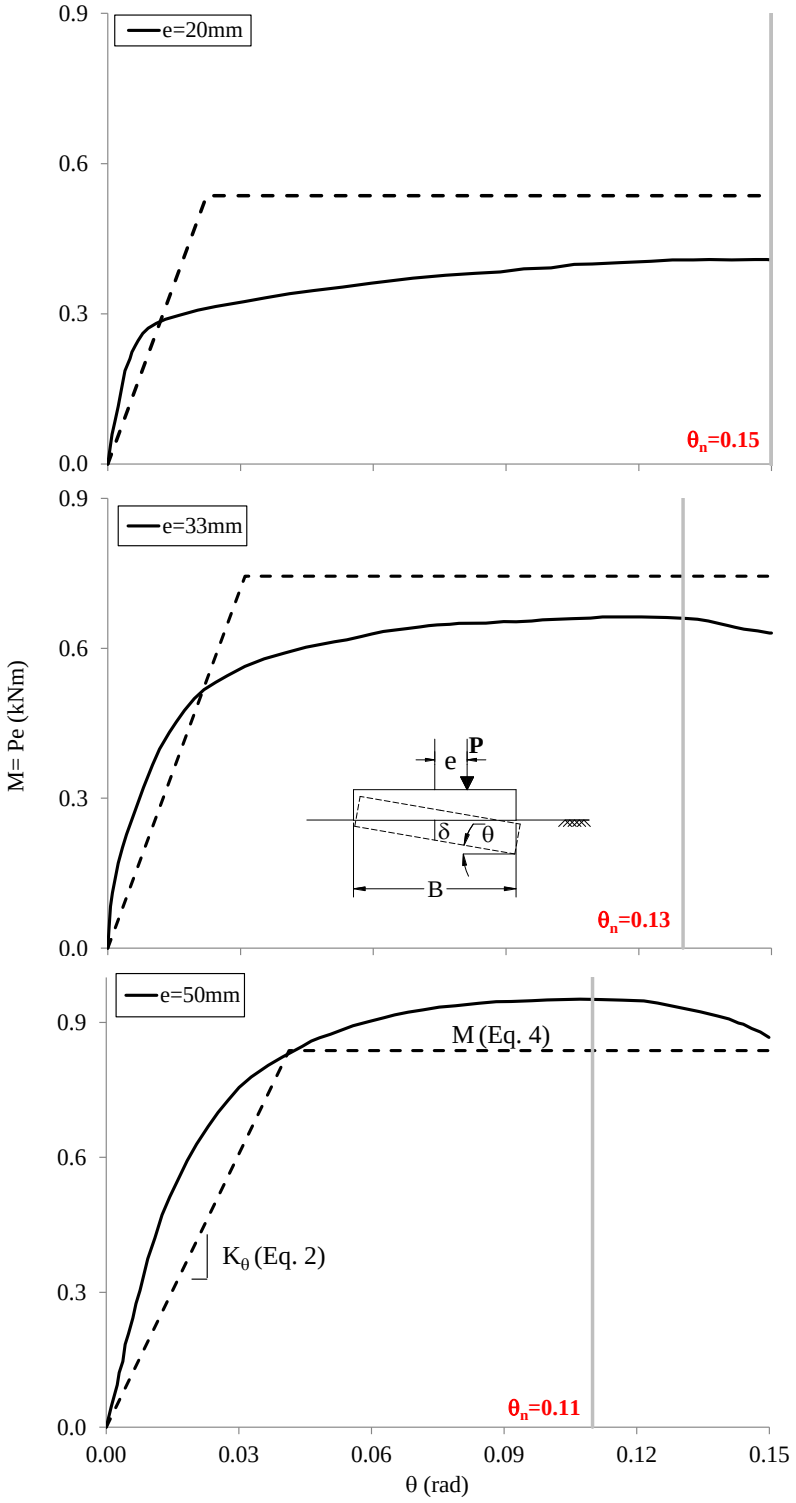

Fig. 9 Moment-rotation response of foundation model under monotonic eccentric loading

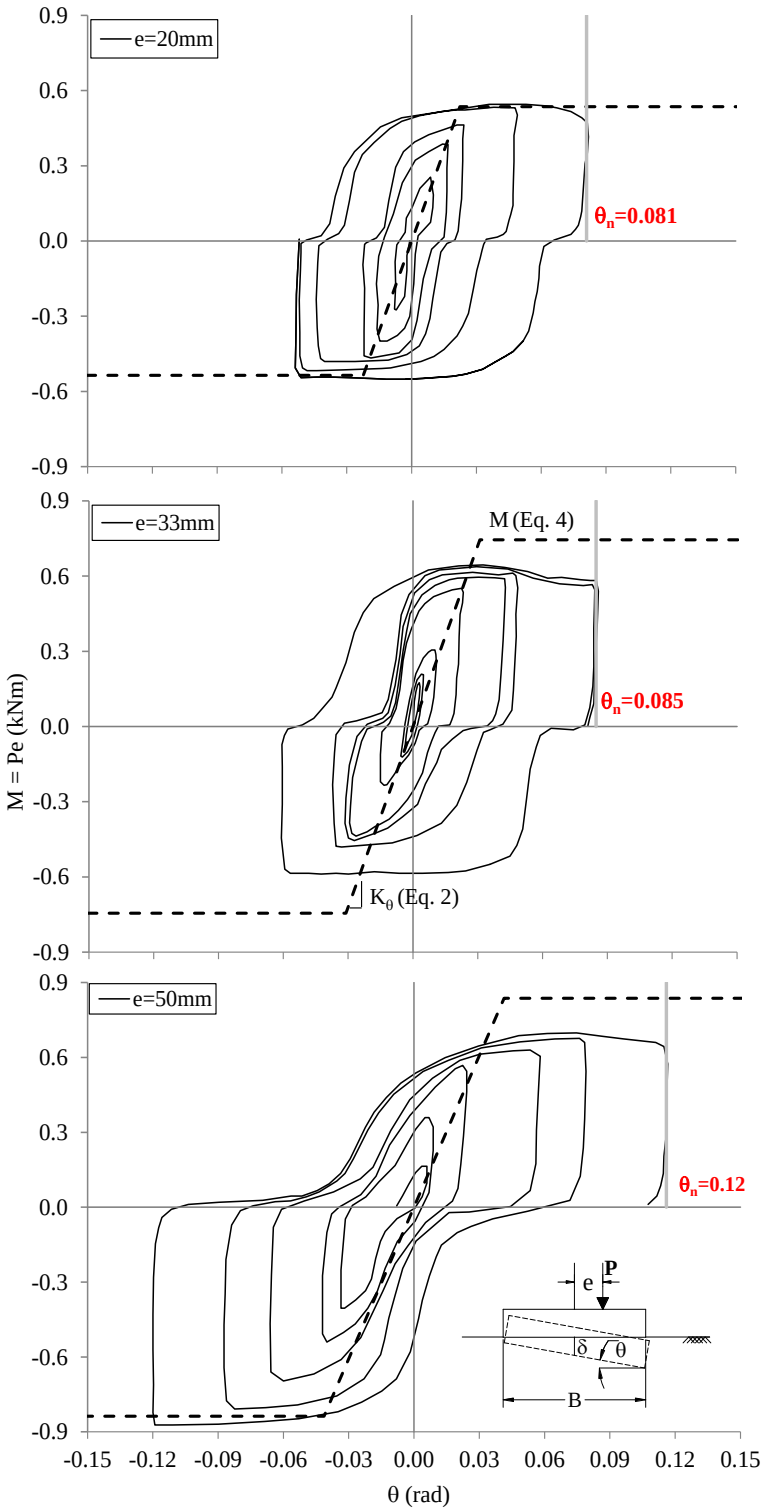

Fig. 10 Moment-rotation response of foundation model under cyclic eccentric loading

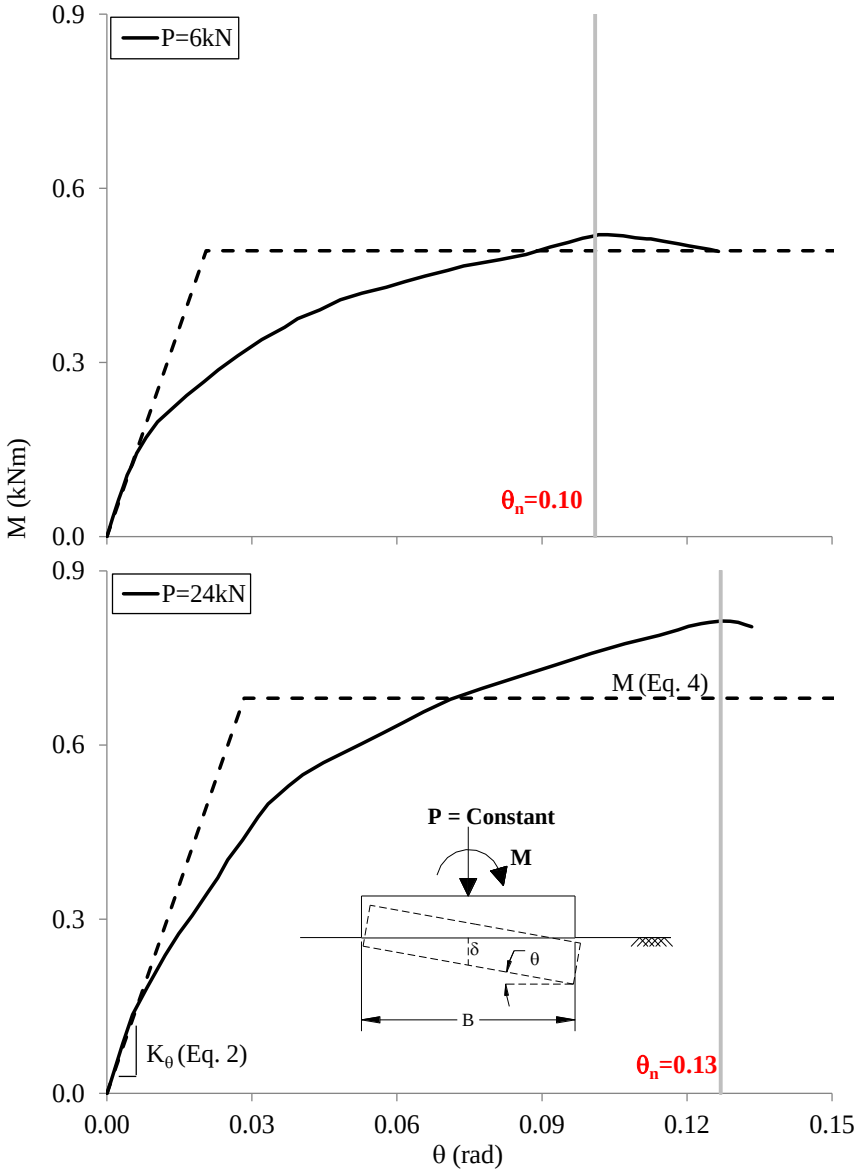

Fig. 11 Moment-rotation response of foundation model under constant axial load and monotonic moment (Rotation readings for P=15 kN test were accidentally lost)

be controlled by the overturning moment rather than axial compression. Because a moment-controlled mode of failure is generally more ductile than a compression-controlled mode of failure, it was first expected that the foundation rotational capacity would increase with the eccentricity of the load. However, no clear trend between the rotational capacity and the eccentricity is observed in Fig. 13 when all results are observed together and, on the contrary, θ_n seems to decrease with the eccentricity for the monotonic tests. A possible explanation of this observation is that large eccentricities are also associated to a greater extent of foundation uplifting and higher

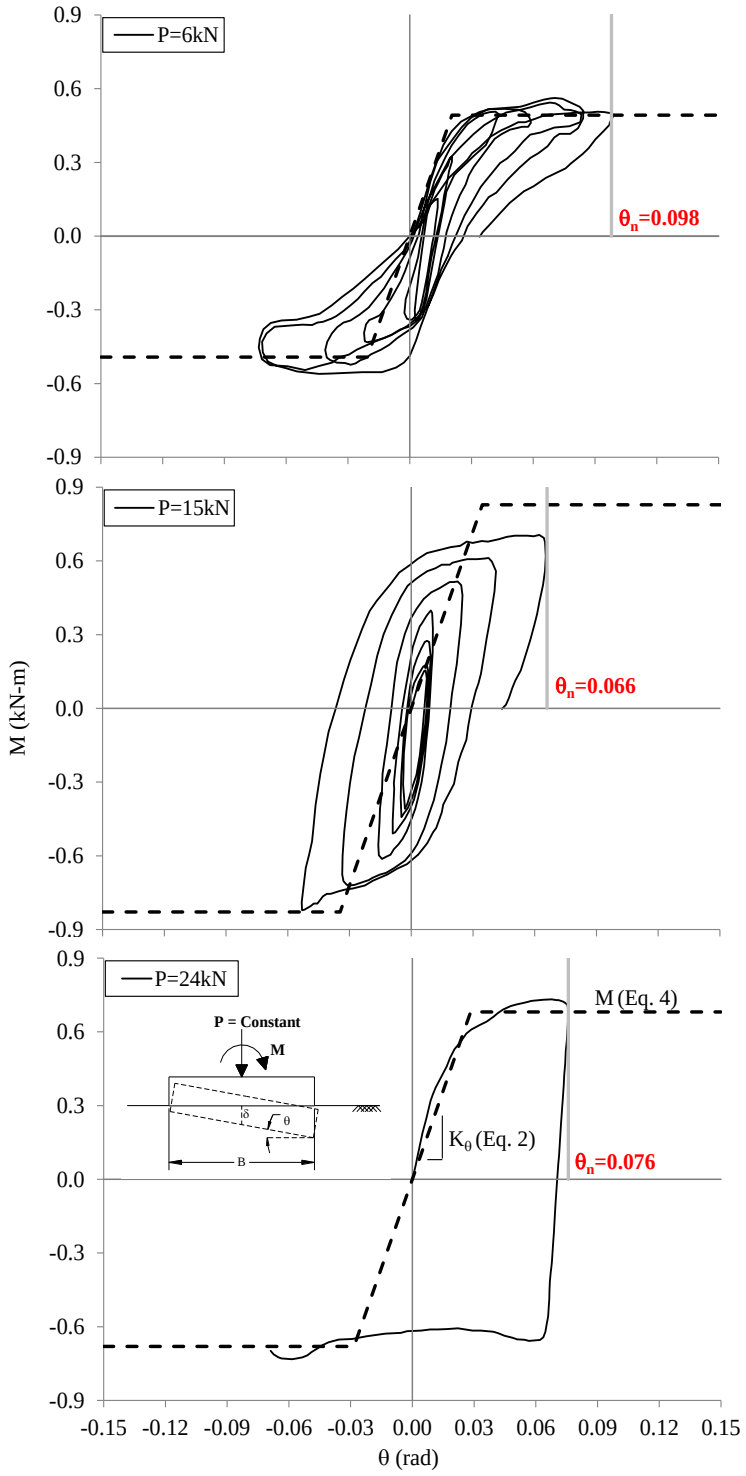

Fig. 12 Moment-rotation response of foundation model under constant axial load and cyclic moment (Further loading cycles were not possible in the P=24 kN test)

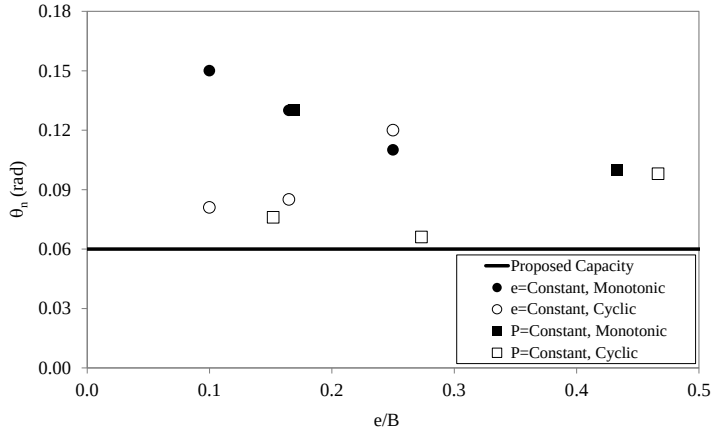

Fig. 13 Foundation rotational capacity versus load eccentricity

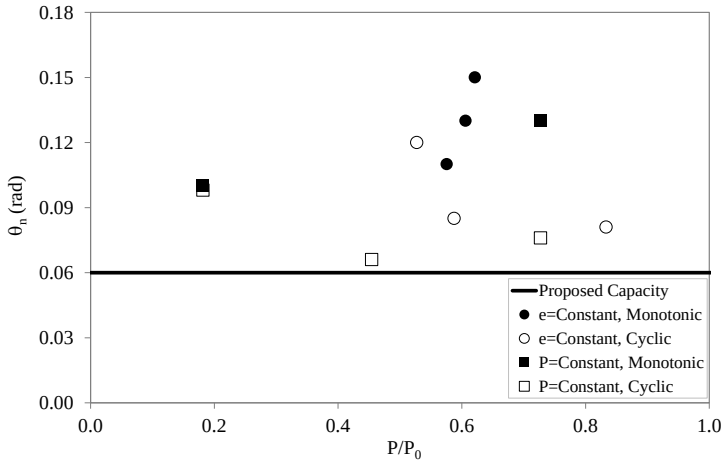

Fig. 14 Foundation rotational capacity versus axial load

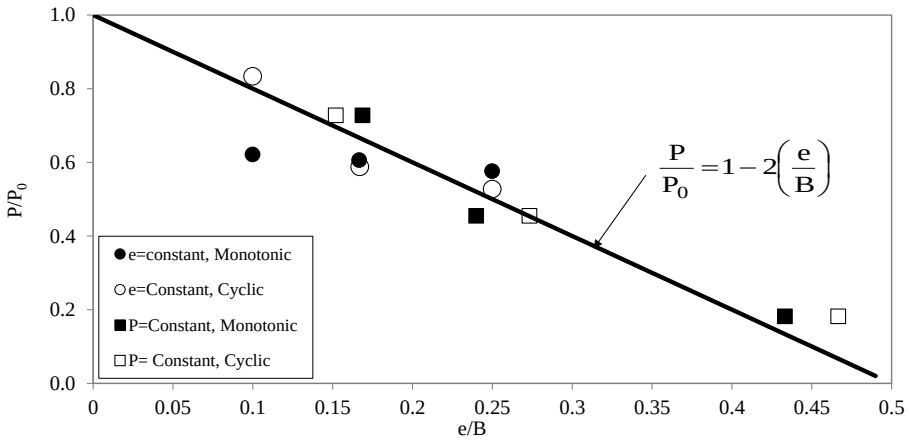

Fig. 15 Foundation normalized axial load capacity versus eccentricity

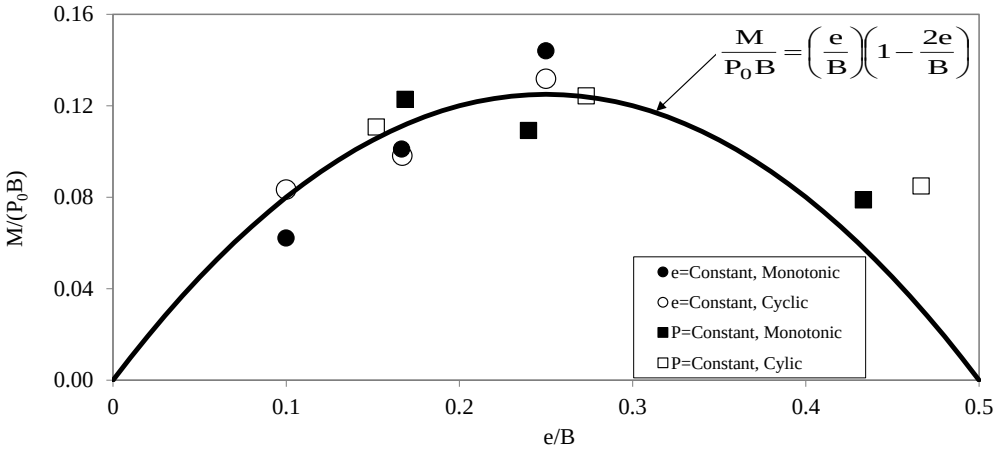

Fig. 16 Foundation normalized moment capacity versus eccentricity

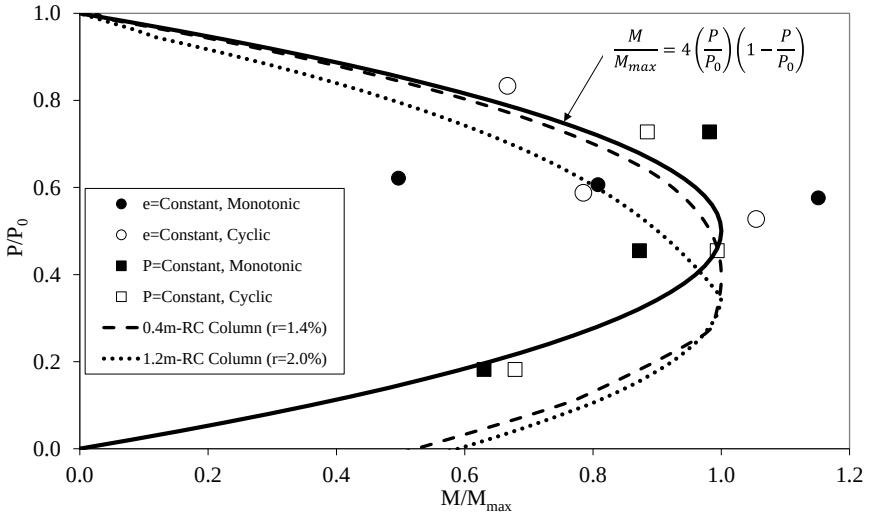

Fig. 17 Foundation normalized interaction (MP) diagram in comparison to reinforced concrete members

concentration of stresses on the compression side, which can translate into a less ductile response.

Fig. 14 indicates that the rotational capacity decreases for extreme (low and high) axial loads. Coincidentally when the applied axial load equals half of the concentric load capacity of the foundation, the theoretical moment capacity (given by Eq. (4b)) reaches its maximum value. It is plausible that for low P/P_0 values the onset of uplifting tends to occur more frequently and thus pinching would limit the energy dissipation capability of the foundation; whereas for high P/P_0 values the moment-rotation response is more compression-controlled and thus less ductile.

Comparisons of Eqs. (3) and (4a) with measured eccentric axial load capacity and measured peak moment capacity of the foundation model are provided in Figs. 15 and 16 respectively. In both cases, the normalization is performed using the concentric axial load capacity obtained from the monotonic test of Series I (Fig. 6), i.e., P_0=33 kN. Although these two figures are just

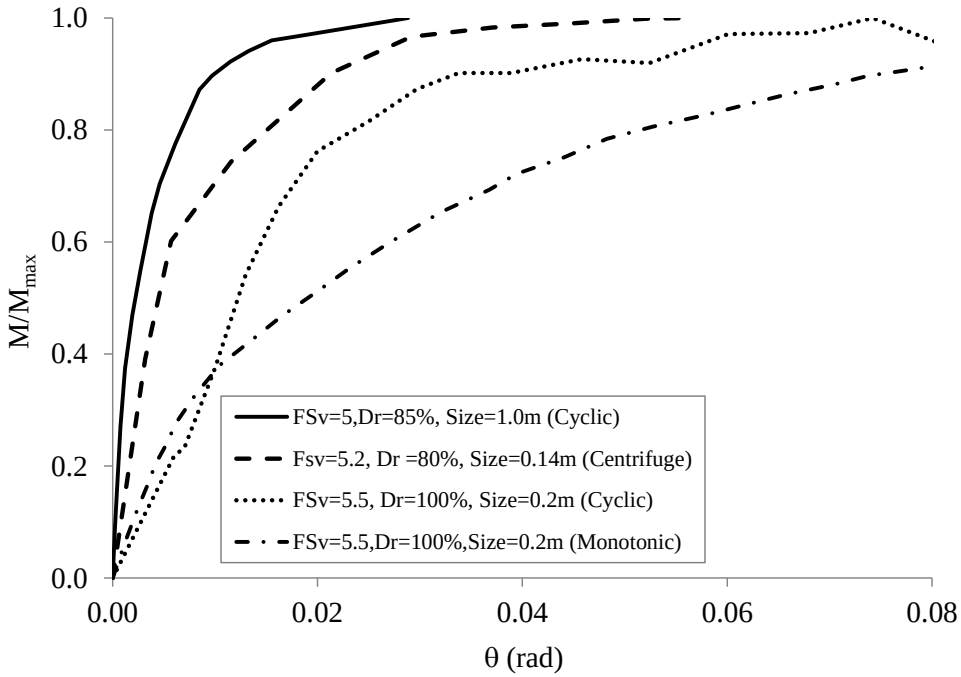

Fig. 18 Measured M-θ envelopes for foundation models with similar test conditions

alternative forms of representing the combined axial load and moment capacity of shallow foundations, they support the fact that the classic equivalent width concept proposed by Meyerhof (1953) produces reasonable estimates of measured values despite its simplicity.

Foundation axial load versus moment capacity envelope (M-P) can be better expressed in terms of normalized variables in order to permit the comparison with the capacity of structural members. Noticing that the maximum moment capacity that can be obtained from Eq. (4b) is $M_{max}=P_0B/8$, the same equation can be re-written as

$$\frac{M}{M_{max}} = 4\frac{P}{P_0}\left(1-\frac{P}{P_0}\right) \tag{5}$$

Eq. (5) is shown in Fig. 17 with a continuous line together with the moment and axial load capacity pairs measured in Series II and III. The relation is theoretically independent of the soil type, and the loading path to failure; either the axial load is constant and the moment varies up to failure, or the axial load is varied and the eccentricity is constant. It is important to mention that the normalized interaction diagram has a similar shape of that for a reinforced-concrete (R/C) or steel member, except that in absence of axial compression the moment capacity is zero because of the inability of the soil to resist tension. The calculated interaction (M-P) diagram for a small 0.4m-square RC column with r=1.4% longitudinal reinforcement ratio and a large 1.2 m-square RC column with r=2.0% longitudinal reinforcement ratio are also included in Fig. 17 for comparison. The 28-day concrete compressive strength was taken as 35 MPa in both cases, while the reinforcement had an assumed yielding stress of 420 MPa (grade 60). Column capacity was

determined using strain compatibility and a conventional limiting concrete compressive strain of 0.003.

5. Benchmarked foundation rotational capacity

Since the measured foundation rotational capacity did not show any clear trend with eccentricity or axial load (Figs. 13-14), a constant rotational capacity of 0.06 rad is proposed for the foundation model tested in this study. Because scale effects cannot be assessed using the information available in the experimental program, it is meaningful to benchmark the proposed rotational capacity against results available in the literature for similar conditions. Two studies were found involving sandy soils compacted to high relative density and foundations subjected to moment cycles and constant axial load. One of the reference studies (Negro *et al*. 2000), known as TRISEE (3D Side Effects of Soil-foundation Interaction in Earthquake and Vibration Risk Evaluation), involved a 1.0 meter square foundation model on Ticino Sand (D_{50}=0.55 mm; coefficient of uniformity, C_u=1.6; specific gravity, G_s=2.68; e_{min}=0.58, e_{max}=0.93). The foundation was subjected to displacement-controlled cycles of overturning moment and a constant axial load of P=300 kN, which corresponded to an estimated FSv=5.0. The relative density of the soil sample of interest was Dr=85%. The other benchmark study was part of a series of centrifuge experiments on scaled (1:20) shear-wall-and-shallow-foundation models conducted at the NEES facility of the University of California (UC) at Davis (Gajan *et al*. 2003). The footing dimension in the direction of the excitation was 140 mm (2.8 m prototype) and was supported on Nevada Sand (D_{50}=0.15 mm) with a relative density Dr=80%. The constant axial load was such that FSv=5.2.

Moment-rotation envelopes (connecting peak values from cycles) of the TRISEE and the UC-Davis tests are shown in Fig. 18 together with the results for the monotonic and cyclic tests with P=6 kN (FSv=5.5) of Series III. In each case the moment ordinate was normalized by the measured maximum moment to permit the comparison of test models of different scale. Although no definite conclusion can be drawn because the foundation models in the evaluated studies were not subject to sufficiently large cycles leading to a decay of the applied moment, it seems plausible that the proposed rotational capacity of 0.06 rad could have been reached in the centrifuge tests performed at UC-Davis. The large-scale TRISEE tests, on the other hand, seem to still have reserve moment (slope of the response is still appreciably positive) and thus rotational capacity beyond the measured 0.025-0.03 rad. It will, nevertheless, be shown in a succeeding section that calculated rotational demands on vulnerable foundations of a structure under major ground excitation are much less than the rotational capacities observed in Fig. 18.

6. Simplified foundation rocking model

Standard ASCE 41-06 defines four levels of analysis to be used in the design of seismic rehabilitation strategies for buildings: linear static (LSP), linear dynamic (LSP), nonlinear static (NSP), and nonlinear dynamic procedures (NDP). Nonlinear procedures are suitable for any type of rehabilitation strategy and require consideration of soil-structure interaction effects by using elastoplastic relations at the base of columns/walls. Upper and lower bounds, expected to contain the actual foundation response, are defined using the best estimate of the foundation stiffness and

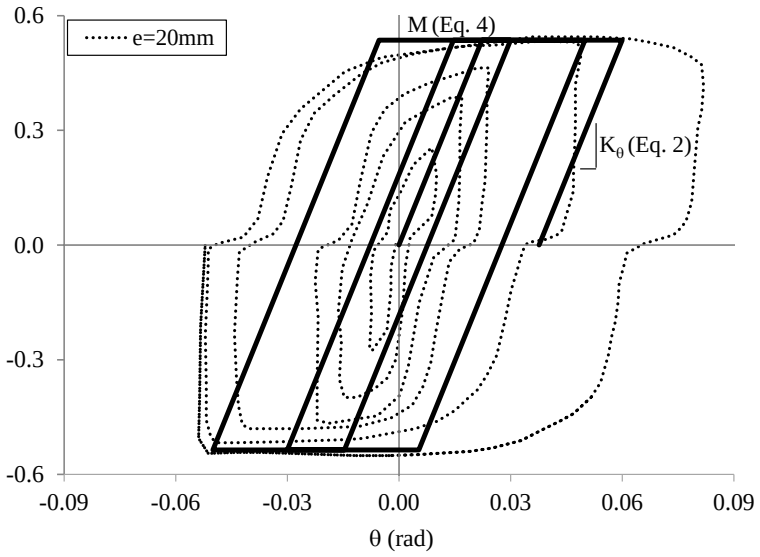

Fig. 19 Simplified moment-rotation for rocking response of foundations

Table 2 Selected ground motion records

Record	Earthquake Name	Year	Station name	Mag.(M_W)	Distance(km)	NEHRP Site
1	Imperial Valley(AS), USA	1979	Calipatria Fire Station	6.5	23.2	D
2	Imperial Valley(AS), USA	1979	Delta	6.5	22	D
3	Imperial Valley(AS), USA	1979	El Centro Array#1	6.5	19.8	D
4	Imperial Valley(AS), USA	1979	El Centro Array#13	6.5	22	D
5	Superstition Hills(AS), USA	1987	Wildlife Liquef. Array	6.5	23.9	D
6	Loma Prieta, USA	1989	Agnews State Hospital	6.9	24.3	D
7	Loma Prieta, USA	1989	Anderson Dam(Downstream)	6.9	19.9	C
8	Loma Prieta, USA	1989	Andersan Dam(L Abut)	6.9	19.9	C
9	Loma Prieta, USA	1989	Coyote Lake Dam(SW Abut)	6.9	20	C
10	Loma Prieta, USA	1989	Gilroy Array #7	6.9	22.4	D
11	Loma Prieta, USA	1989	Hollister – SAGO Vault	6.9	29.5	C
12	Northridge, USA	1994	Castaic – Old Ridge Route	6.7	20.1	C
13	Northridge, USA	1994	LA – Baldwin Hills	6.7	23.5	D
14	Northridge, USA	1994	LA – Centinela St	6.7	20.4	D
15	Northridge, USA	1994	LA – Cypress Ave	6.7	29	C
16	Northridge, USA	1994	LA – Fletcher Dr	6.7	25.7	C

Table 2 Continued

17	Northridge, USA	1994	LA – N Westmoreland	6.7	23.4	D
18	Northridge, USA	1994	LA – Pico & Sentous	6.7	27.8	D
19	Kobe, Japan	1995	Abeno	6.9	24.9	D
20	Kobe, Japan	1995	Kakogawa	6.9	22.5	D
21	Kobe, Japan	1995	Morigawachi	6.9	24.8	D
22	Kobe, Japan	1995	OSAJ	6.9	21.4	D
23	Kobe, Japan	1995	Sakai	6.9	28.1	D
24	Kobe, Japan	1995	Yae	6.9	27.8	D

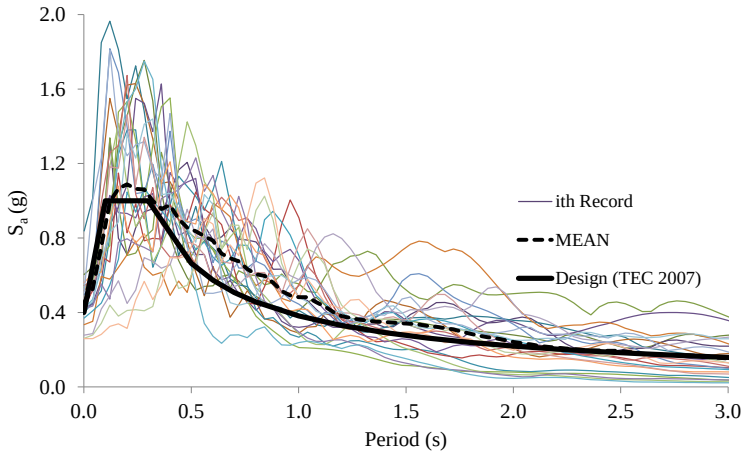

Fig. 20 Acceleration response spectra for selected ground motions

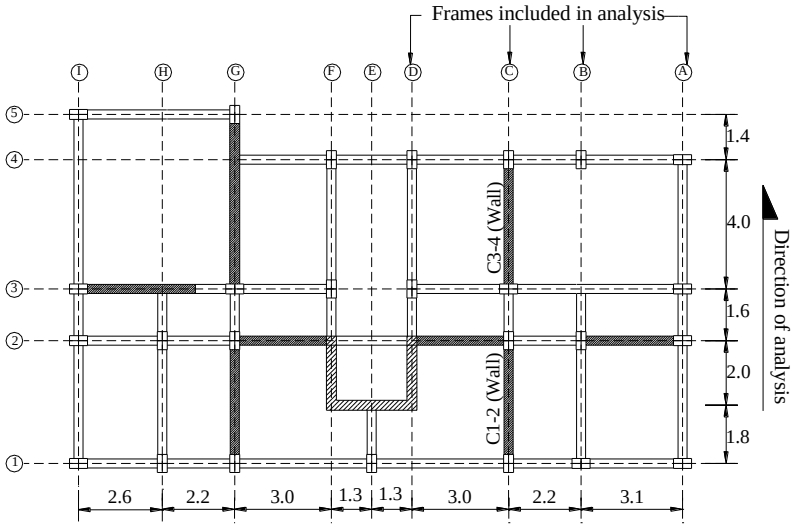

Fig. 21 Plan view of 8-story structure

Table 3 Model parameters for 8-story building example

		Column/Wall		Foundation						
		Axial Load at Column/Wall Base, P	Moment Capacity at Base	B	L	K_{s0}	Settlement under P	K_θ	Moment Capacity, M	$\theta_y=M/K_\theta\mu_\theta=0.06/\theta_y$
Frame[1]	Member	(kN)	(kN-m)	(m)	(m)	(kN/m^3)	(mm)	(kN-m)	(kN-m)	(rad)	(N/A)
A	A1	230	55	2.0	1.0	3.83E+04	3.0	2.55E+04	200	7.8E-03	7.7
	A2	330	60	2.0	1.0	3.83E+04	4.3	2.55E+04	270	1.1E-02	5.7
	A3	340	60	2.0	1.0	3.83E+04	4.4	2.55E+04	270	1.1E-02	5.7
	A4	160	55	2.0	1.0	3.83E+04	2.1	2.55E+04	150	5.9E-03	10.2
B	B1	400	60	2.5	1.0	3.63E+04	4.4	4.72E+04	410	8.7E-03	6.9
	B2	560	190	2.5	1.5	3.63E+04	4.1	7.08E+04	580	8.2E-03	7.3
	B4	420	170	2.5	1.0	3.63E+04	4.6	4.72E+04	420	8.9E-03	6.8
C	**C1-2***	940	3500	4.0	1.5	3.34E+04	4.7	2.67E+05	1530	5.7E-03	10.5
	C3-4*	980	3500	4.0	1.5	3.34E+04	4.9	2.67E+05	1580	5.9E-03	10.1
D	D1-2*	1000	620	4	1.5	3.34E+04	5.0	2.67E+05	1608	6.0E-03	10.0
	D3	620	170	2.5	1.5	3.63E+04	4.6	7.08E+04	620	8.8E-03	6.9
	D4	440	170	2.5	1.0	3.63E+04	4.9	4.72E+04	440	9.3E-03	6.4

1Note: refer to Figs. 20 and 21
*: Shear Walls

strength multiplied by factors of 2.0 and 0.5 respectively (Fig. 1). Design forces at the base of columns/walls are generally obtained using the upper bound values for the foundation stiffness and strength; whereas lower bound values produce maximum drift demands. The significant difference between these bounds (a factor of four) reflects the level of uncertainly on soil properties that could be expected in consulting practice and the quality of information that may be available to the designer.

Following the simplified philosophy of current design standards, an equivalent elasto-plastic moment-rotation model with kinematic hysteresis, such as that shown Fig. 19, is used to model a building with vulnerable foundations and preliminarily evaluate the implication of a finite rotational capacity. The measured moment-rotation response for the cyclic e=20 mm test is shown in the same figure for comparison with the corresponding simplified foundation rocking model.

7. Building with vulnerable foundations under seismic scenario

In order to examine the practical implication of a limited rotational capacity in a building with vulnerable foundations, a numerical example was performed. Base excitation consists of the 24 far-fault ground motions listed in Table 2, which correspond to a seismic scenario with the following hazard conditions:

- Moment magnitude: Mw=6.7±0.2
- Joyner-Boore distance: RJB=25±5 km
- NEHRP soil type: C or D
- Highest usable period ≥4 sec

Fig. 20 shows the mean 5%-damping response spectra of scaled ground motions together with the 475-year return-period design spectra from the Turkish Earthquake Code (TEC 2007) for Zone 1 and Site Class 2 (equivalent to Site Class C in NEHRP). Scale factors, corresponding to the fundamental period of the structure with flexible supports, were obtained using a modified version of the ASCE/SEI 7-10 procedure that was proposed by Reyes and Chopra (2012).

The structure consists of an 8-story reinforced concrete building located in the city of Ceyhan-Turkey that was strengthened with reinforced concrete shear walls (Gur 1999). The typical floor area is 227 m^2 and the story height is 3.0 m (Fig. 21). Columns are rectangular with as-built dimensions of 0.25×0.60 m; beams are 0.20×0.60 m; and reinforced concrete shear walls are 0.25 m thick. The compressive strength of concrete was only 12MPa as measured from actual concrete cores; whereas the specified yielding stress of the reinforcing steel was also rather low and equal to 220 MPa. The amount of longitudinal reinforcement in columns and walls was assumed equal to 1.0 and 0.25 percent of the cross-sectional area.

It was hypothetically assumed that the supporting soil for the building was identical to that in the experimental program of this study, which was characterized using the results of the monotonic test under concentric loading shown in Fig. 6. This provides an ultimate bearing capacity σ_0=0.85 MPa and an initial subgrade modulus K_{s0}=36 MPa/0.2 m=180 MPa/m. Based on an assumed total floor weight (including live load) of 10 kN/m^2 and a minimum factor of safety for vertical load of five (FSv=5.0), plausible foundation sizes were selected as summarized in Table 3.

In order to account for size effects in cohensionless soils, the subgrade modulus for any footing of size B, K_{s0}, was estimated based on the subgrade modulus for a 0.3-m standard plate, K^*_{s0}, by a using semi-empirical equation proposed by Terzaghi (1955)

$$K_{s0} = K^*_{s0}\left(\frac{B+0.30m}{2B}\right)^2 \tag{6}$$

Application of this equation to the conditions of the test soil (B=0.2 m and K_{s0}=180 MPa/m) provided the subgrade modulus for a standard plate of K^*_{s0}=115 MPa/m. This value was in turn used to estimate K_{s0} for all selected foundation sizes of the building (Table 3). Short-term gravity load settlements, calculated based on the values of K_{s0}, were found to be less than 5 millimeters and thus confirming that foundation sizing is controlled by the bearing capacity of the soil rather than its stiffness.

Simplified elastoplastic foundation rocking models were constructed by using the rotational stiffness, K_θ, calculated from Eq. (2a) and the moment capacity, M, calculated from Eq. (4b). It was assumed that the foundations lose their ability to sustain moment when the rotation demand reaches the limiting value of 0.06 rad.

The axial load on each foundation, P, was taken constant and equal to that at the base of column/wall under gravity load alone. The simplified nature of the elastoplastic foundation model does not justify the definition of a failure surface to account for axial load variations during ground excitation. Foundation yielding rotations, θ_y, and the rotational ductility capacity, μ_θ, are also included in Table 3. The former was calculated as the ratio of the moment capacity to the rotational stiffness of the foundation, whereas the latter was calculated as the ratio of the rotational capacity (0.06 rad) and the yielding rotation.

Moment capacities for structural member were determined by strain compatibility using a conventional limiting concrete compressive strain of 0.003. As observed in Table 3, foundations under the columns cannot yield because their moment capacity exceeds that of the supported

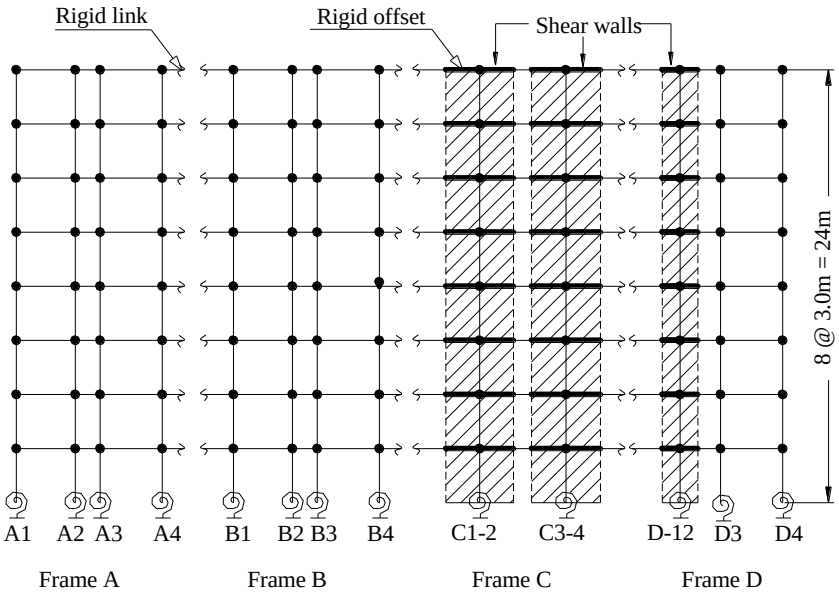

Fig. 22 Numerical modeling of 8-story structure

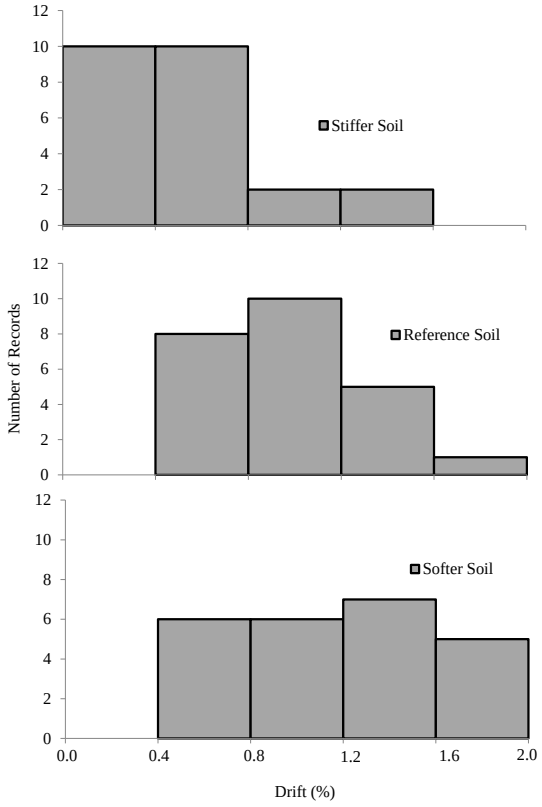

Fig. 23 Histogram of maximum interstory drift ratio

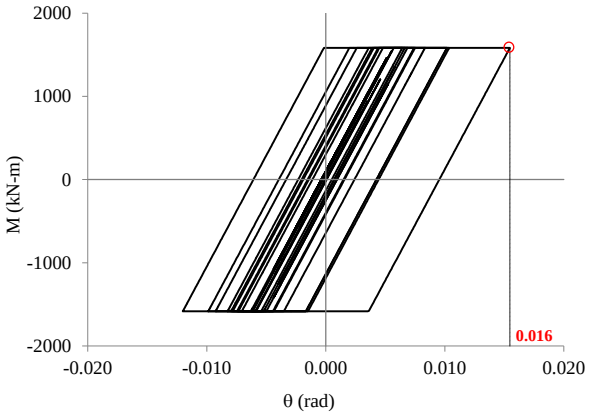

Fig. 24 Moment-rotation response of foundation under shear wall C3-4 for record#11 and Reference Soil

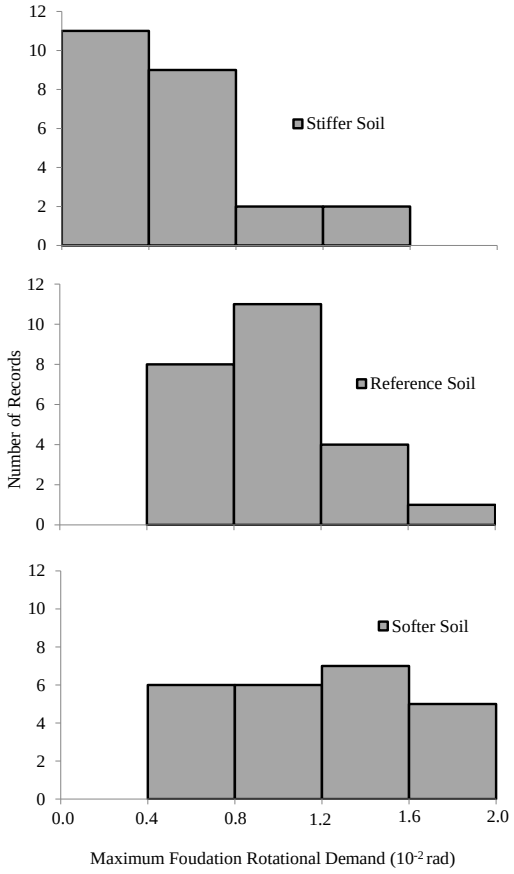

Fig. 25 Histogram of maximum foundation rotation demand

structural element. However, shear walls C1-2 and C3-4 (Fig. 21) have flexural capacities that far exceed the moment capacities of their supporting foundations. This means that under major ground

excitation, the foundations under these main lateral load resisting elements are vulnerable and thus prone to uplifting and yielding.

Numerical modelling of the building was performed using the computer program SAP2000® version 15. It was assumed that the floor slabs provide full diaphragm action, and that proper reinforcement detailing precludes the occurrence of brittle modes of failures in shear or anchorage loss. Because of the approximately symmetrical configuration of the structure, only frames A through D (Fig. 21) were considered in the two-dimensional model (Fig. 22). The finite element model accounts for the formation of plastic hinges in flexure at ends of columns and walls coupled with the elasto-plastic rocking behavior of the foundations.

The lowest period of vibration in the direction of analysis was calculated to be 0.96s and the corresponding modal mass participation was 83%. Nonlinear modal time histories analyses of the building model under the scaled ground records were performed assuming a constant damping ratio of 5% and considering twelve modes, which provided a 99% mass participation ratio. The building's mass was lumped at the floors.

Histograms of the computed maximum nonlinear interstory drift ratios for the model with vulnerable foundations are summarized in Fig. 23.

Lower and upper bound foundation models, defined by using half and twice the rotational stiffness and moment capacity, were also considered in the analyses thus requiring additional sets of nonlinear time-history calculations. These boundary foundation conditions are referred to as Softer Soil and Stiffer Soil, whereas the foundations parameters listed in Table 3 (K_θ and M) correspond to the Reference Soil. As expected, the lower bound soil conditions produce larger drift ratios but the difference with the upper bound is not significant. This observation suggests that trying to define a detailed/realistic soil-foundation model is not necessary productive for this example.

The absolute maximum calculated interstory drift was 1.7%, which could cause excessive damage and/or collapse to non-structural elements but would typically be associated to moderate damage of structural elements that are properly detailed. This implies that the presence of vulnerable foundations does not necessarily compromise the structural integrity of the building provided that loss of bearing capacity of foundations does not occur.

Fig. 24 shows the calculated moment-rotation response for a foundation under wall C3-4 when the building model is supported on the Reference Soil while being subjected to ground motion #11 (Table 2). It can be observed that although the moment capacity of the foundation is reached, the corresponding maximum rotational demand (0.016 rad) is only a fraction of the limiting rotational capacity (0.06 rad).

Histograms of the calculated maximum foundation rotational demands are shown in Fig. 25 for the Reference Soil and also for the upper and lower soil property boundaries defined above. Once again, the maximum rotation demand is larger for the Softer Soil but still a fraction of the limiting rotational capacity. This suggests that soil plastification can indeed occur but foundation loss of bearing capacity is highly unlikely, even if soil nonlinearity at small level of settlements/rotations was modelled. Therefore, yielding of the soil can potentially be a reliable source of energy dissipation for the soil-structure system considered in this example.

8. Conclusions

This paper presents the results of an experimental program aimed at investigating the

deformation capacity of foundation models on a cohesionless soil. For the particular case of 200-mm square rigid footings on a well-compacted but poorly graded sand, the rotational capacity was measured to be at least 0.06 rad and did not appear to depend on the eccentricity of the load but was higher when the applied axial load approached one half of the concentric load capacity of the foundation. Moment-rotation cycles were wide and stable, thus suggesting that soil-foundations may intrinsically be a reliable source of energy of dissipation to soil-structure systems. For low axial loads, the moment rotation response tended to be more pinched as a result of loss of contact between portions of the foundation and the supporting soil.

Foundation bearing capacity under eccentric loading was found to comply well with Meyerhof's equivalent width concept by which the eccentric capacity of a shallow foundation can be estimated based on its concentric bearing capacity. Results from a numerical model of an 8-story building with vulnerable foundations showed that the calculated maximum rotation demands were much less than the foundation rotational capacity measured in the experimental program of this study, thus supporting the notion that, for a similar soil conditions, foundations may dissipate energy through soil yielding without losing their ability to transfer loads. Research is needed to evaluate dynamic effects, such as number of cycles and loading rate, on the deformation capacity of shallow foundations. Furthermore, evaluation of size effects is required to develop realistic performance limit states which can be used to supplement current design/assessment provisions.

References

ASCE/SEI 41-06 (2007), *Seismic rehabilitation of existing buildings*, *Am. Soc. of Civ. Eng*., Reston, VA, USA.

Briaud, J.L. and Guibbens, R. (1994), "Predicted and measured behavior of five spread footings on sand", *Settlement '94 ASCE conference at Texas A&M University*, College Station.

Briaud, J.L. and Gibbens, R. (1999), "Behavior of five large spread footings in sand", *J. Geotech. Geoenvir. Eng.*, **125**(9), 787-796.

Chatzigogos, C.T., Pecker, A. and Salençon, J. (2009), "Macroelement modeling of shallow foundations", *Soil Dyn. Earthq. Eng*., **29**(5), 765-781.

Consoli, N.C., Schnaid, F. and Milititsky, J. (1998), "Interpretation of plate load tests on residual soil site", *J. Geotech. Geoenvir. Eng.*, **124**(9), 857-867.

Cremer, C., Pecker, A. and Davenne, L. (2001), "Cylic macro-element for soil-structure interaction: material and geometric nonlinearities", *Int. J. Numer. Anal. Meth. Geomech.*, **25**(13), 1257-1284.

Gajan, S., Phalen, J. and Kutter, B. (2003), "Soil-foundation structure interaction: Shallow foundations: Centrifuge data report for the SSG03 test series", Center for Geotechnical Modeling Data Report UCD/CGMDR-03/02.

Gajan, S., Hutchinson, T.C., Kutter, B., Raychowdhury, P., Ugalde, J.A. and Stewart, J.P. (2008), "Numerical models for the analysis and performance-based design of shallow foundations subjected to seismic loading", PEER Data Rep. No. 2007/04, Pacific Earthq. Eng. Res. Center, Berkeley, CA.

Gajan, S., Raychowdhury, P., Hutchinson, T.C., Kutter, B.L. and Stewart, J.P. (2010), "Application and validation of practical tools for nonlinear soil-foundation interaction analysis", *Earthq. Spectra*, **26**(1), 111-129.

Grange, S., Kotronis, P. and Mazars, J. (2009), "A macro-element to simulate dynamic soil-structure interaction", *Eng. Struct*., **31**(12), 3034-3046.

Gur, T. (1999), "Capacity evaluation of damaged and repair structures", M.S Thesis, Middle East Technical University, Ankara, Turkey.

Hall, J.R. Jr. (1967), "Coupled rocking and sliding oscillations of rigid circular footings", *Int. Symposium on*

Wave Propagation and Dynamics Properties of Earth Materials, Albuquerque.
Harden, C.W. and Hutchinson, T.C. (2009), "Beam-on-nonlinear-Winkler-foundation modeling of shallow, rocking-dominated footings", *Earthq. Spectra*, **125**(2), 277-300.
Lamb, H. (1904), "On the propagation of tremors over the surface of elastic solid", *Phil Trans. Roy. Soc. London*, **203**, 1-42.
Meyerhof, G.G. (1953), "The bearing capacity of footings under eccentric and inclined loads", *Proceedongs of the Third International Conference of Soil Mechanics and Foundation Engineering*, Switzerland.
Negro, P., Paolucci, R., Predetti, S. and Faccioli, A.E. (2000), "Large-scale soil structure interaction experiments on sand under cyclic loading", *Proceedings of 12th World Conference of Earthquake Engineering*, Auckland, New Zeland.
Pais, A. and Kausel, E. (1988), "Approximate formulas for dynamic stiffnesses of rigid foundations", *Soil Dyn. Earthq. Eng.*, **7**(4), 213-227.
Parmelee, R.A. (1967), "Building-foundation interaction effect", *J. Eng. Mech. Div.*, **93**(EM2), 131-152.
Parmelee, R.A., Perelman, D.S., Lee, S.L. and Keer, M.L. (1968), "Seismic response of structure-foundation systems", *J. Eng. Mech. Div.*, **94**(EM6), 1295-1315.
Raychowdhury, P. (2008), "Nonlinear winkler-based shallow foundation model for performance assessment of seismically loaded structures", Ph.D. Dissertation, University of California, San Diego.
Reyes, J.C. and Chopra, A.K. (2012), "Modal pushover-based scaling of two components of ground motion records for nonlinear RHA of buildings", *Earthq. Spectra*, **28**(3), 1243-1267.
Smith-Pardo, J.P. and Bobet, A. (2007), "Behavior of rigid footings on gravel under axial load and moment", *J. Geotech. Geoenvir. Eng.*, **133**(10), 1203-1215.
Smith-Pardo, J.P. (2008), "Reinforced concrete walls with vulnerable foundations", *J. Geotech. Geoenvir. Eng.*, **134**(2), 257-261.
TEC (2007), *Specifications for Structures to be Built in Disaster Areas (TEC 98/07)*, *Ministry of Public Works and Resettlement*, Ankara, Turkey.
Terzaghi, K. (1955), "Evaluation of coefficients of subgrade reaction", *Géotechnique*, **5**(4), 297-326.
Ugalde, J.A, Kutter, B.L. and Jeremic, B. (2010), "Rocking response of bridges on shallow foundations", PEER Rep. No. 2010/101, Pacific Earthq. Eng. Res. Center, Berkeley, CA.
Winkler, E. (1867), *Die Lehre von der Elastizitat und Festigkeit*, Dominicus, Prague.

JL